JACS
JOURNAL OF THE AMERICAN CHEMICAL SOCIETY

pubs.acs.org/JACS

Article

Catalytic Activity of *trans*-Bis(pyridine)gold Complexes

Ann Christin Reiersølmoen, Dániel Csókás, Sigurd Øien-Ødegaard, Alan Vanderkooy, Arvind Kumar Gupta, Anna-Carin C. Carlsson, Andreas Orthaber, Anne Fiksdahl, Imre Pápai,* and Máté Erdélyi*

Cite This: *J. Am. Chem. Soc.* 2020, 142, 6439−6446

Read Online

ACCESS | Metrics & More | Article Recommendations | Supporting Information

ABSTRACT: Gold catalysis has become one of the fastest growing fields in chemistry, providing new organic transformations and offering excellent chemoselectivities under mild reaction conditions. Methodological developments have been driven by wide applicability in the synthesis of complex structures, whereas the mechanistic understanding of Au(III)-mediated processes remains scanty and have become the Achilles' heel of methodology development. Herein, the systematic investigation of the reactivity of bis(pyridine)-ligated Au(III) complexes is presented, based on NMR spectroscopic, X-ray crystallographic, and DFT data. The electron density of pyridines modulates the catalytic activity of Au(III) complexes in propargyl ester cyclopropanation of styrene. To avoid strain induced by a ligand with a nonoptimal nitrogen−nitrogen distance, bidentate bis(pyridine)−Au(III) complexes convert into dimers. For the first time, bis(pyridine)Au(I) complexes are shown to be catalytically active, with their reactivity being modulated by strain.

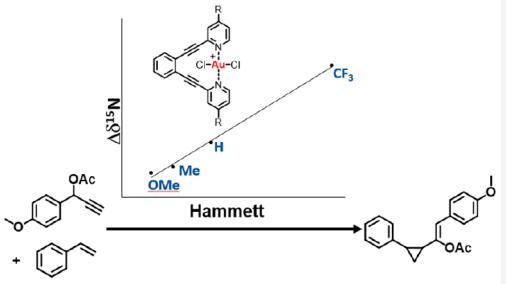

INTRODUCTION

Despite humankind's fascination with gold ever since ancient times, Au catalysis has lagged behind the chemistry of other transition metals, such as palladium, rhodium, and platinum. Recently, significant efforts have been put into the establishment and understanding of Au(I)-catalyzed processes,[1,2] whereas Au(III)-mediated reactions have received only minute interest.[3−5] They have sometimes been simplistically rationalized as Au(I) catalytic processes, with Au(III) being a precatalyst,[6] or as intermediates in a catalytic redox cycle starting with Au(I).[7−10] This lag is likely explained by the challenging lability of Au(III) complexes by the largely unexplored potential of their ligation and by the lack of experimental evidence necessary for understanding of the mechanism of Au(III)-mediated processes.[11] Ligated Au(III) complexes have so far primarily been developed for biological applications,[12] with only scarce examples of catalysts designed for organic reactions.[13−25] Such ligated complexes have been reported to exhibit higher stability and increased catalytic activity as compared to inorganic Au(III) salts. Current ligated Au(III) complexes are typically based on bidentate *cis*-chelating ligands and contain oxazolines,[15,23,26,27] *N*-heterocyclic carbenes,[24,28] aromatic groups,[25,29−31] or salen.[32] *Trans*-chelating ligands have so far barely been studied. Pyridine derivatives, a frequent motif in transition metal chemistry,[33,34] have also been explored for ligation of Au(III)[35−38] and have shown to yield an improved catalytic performance and stability[39] as compared to simpler Au(III) salts, e.g., K/NaAuCl$_4$, AuCl$_3$, and AuBr$_3$, presumably due to activation and stabilization of the Au(III) center. Whereas some initial data exist, the catalytic activity of pyridine complexes has not yet been systematically investigated, and the mechanism of pyridine-ligated Au(III)-mediated reactions remains unexplored. Motivated by this knowledge gap, we studied bis(pyridine)Au(III) complexes, evaluating the influence of electronic and steric effects on their reactivity and investigating their coordination mode by using NMR spectroscopic, X-ray crystallographic, and computational (DFT) techniques.

RESULTS AND DISCUSSION

Bis(pyridine)Au(III) chloride was prepared by addition of 2 equiv of pyridine to a methanol solution of KAuCl$_4$, resulting in immediate precipitation of [(**1**-H)$_2$-Au(III)]Cl (Figure 1 and Table 1). The single set of ^{1}H, ^{13}C, and ^{15}N NMR signals observed for this product was compatible with that previously reported.[40] Complex [(**1**-H)$_2$-Au(III)]Cl readily catalyzed the propargyl ester (**5**) cyclopropanation of styrene (**6**), yielding full conversion within 1 h (Table 1, entry 1). To evaluate the impact of electron density on catalytic activity, the 4-substituted complexes [(**1**-CF$_3$)$_2$-Au(III)]Cl, [(**1**-CH$_3$)$_2$-Au(III)]Cl, and [(**1**-OCH$_3$)$_2$-Au(III)]Cl were also prepared. The electron-poor [(**1**-CF$_3$)$_2$-Au(III)]Cl showed increased catalytic

Received: February 18, 2020
Published: March 13, 2020

https://dx.doi.org/10.1021/jacs.0c01941
J. Am. Chem. Soc. 2020, 142, 6439−6446

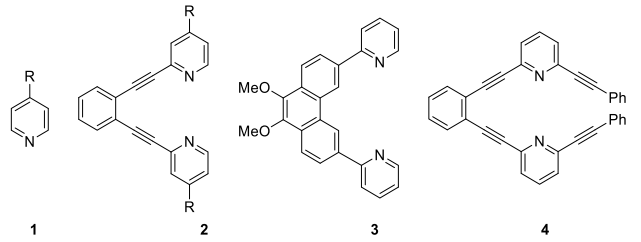

Figure 1. Pyridine-based ligands utilized for Au(I) and Au(III) ligation. Here, R may be H (**1**-H and **2**-H), CF_3 (**1**-CF_3 and **2**-CF_3), CH_3 (**1**-CH_3 and **2**-CH_3), OCH_3 (**1**-OCH_3 and **2**-OCH_3), or asymmetric CH_3/CF_3 (**2**-CH_3/CF_3). Ligands **2**–**4**[41,42] have previously not been utilized in Au-mediated catalysis.

Table 1. Reactivity of the $[(1\text{-R})_2\text{-Au(III)}]^+$ and $[(1\text{-H})_2\text{-Au(I)}]^+$ Complexes in Cyclopropanation[a]

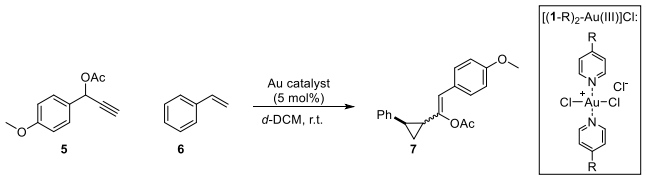

entry	Au catalyst	reaction time	conv [%] (*trans*:*cis*)[b]
1	$[(1\text{-H})_2\text{-Au(III)}]Cl$	1 h	100 (25:75)
2	$[(1\text{-CF}_3)_2\text{-Au(III)}]Cl$	30 min	100 (36:64)
3	$[(1\text{-CH}_3)_2\text{-Au(III)}]Cl$	12 h	83 (17:83)
4	$[(1\text{-OCH}_3)_2\text{-Au(III)}]Cl$	12 h	
5	$[(1\text{-H})_2\text{-Au(I)}]BF_4$	24 h	<5 (<1:>99)

[a]No conversion into product is observed without the presence of an Au catalyst. [b]As this ratio has previously been studied in detail,[11] it is not discussed here.

activity, giving full conversion within 30 min (Table 1, entry 2), most likely as a result of weaker coordination of the ligand. The electron rich-complexes $[(1\text{-CH}_3)_2\text{-Au(III)}]Cl$ and $[(1\text{-OCH}_3)_2\text{-Au(III)}]Cl$ were strongly deactivated (Table 1, entries 3 and 4). ^{15}N NMR chemical shifts provided valuable information about metal coordination strength.[43] The ^{15}N NMR coordination shifts ($\Delta\delta^{15}N_{coord}$) of the $[(1\text{-R})_2\text{-Au(III)}]Cl$ complexes (Table 2) corroborate the electron density dependence of the reactivity. This is further supported by the increased stability (ΔG_{stab}, Table 2) of the more electron-rich complexes, as computed by DFT (for details, see the Supporting Information).

As Au(III) has previously been suggested to show catalytic activity by being a precatalyst for Au(I)-mediated processes, we evaluated the catalytic activity of $[(1\text{-H})_2\text{-Au(I)}]BF_4$ (Table 1, entry 5). Its low activity revealed that the oxidation state of Au(III) plays an important role in the catalysis of the propargyl ester cyclopropanation and that $[(1\text{-H})_2\text{-Au(III)}]Cl$ is highly unlikely to act as a precatalyst for the corresponding Au(I) complex. Calculations predicted the preference of *trans* coordination of **1**-R pyridine ligands in $[(1\text{-R})_2\text{-Au(III)}]^+$complexes, with the *cis* geometries being 1.2–6.3 kcal/mol less stable (see the Supporting Information). This finding is corroborated by the X-ray crystallographic data of bis(pyridine)-type Au(III) complexes.[44] To evaluate whether a *trans*-coordinating ligand may lead to a catalytically active species, we synthesized the geometrically restricted 1,2-bis(4-R-pyridin-2-yl)ethynyl)benzene, **2** (Figure 1 and Scheme 1).

Scheme 1. Formation of the Au(I) and Au(III) Complexes of Ligand 2-H and the Au(III) Complexes of Its 4-Substituted Analogues, 2-R, Where R Is H (2-H), CF_3 (2-CF_3), CH_3 (2-CH_3), OCH_3 (2-OCH_3), or Both CH_3 and CF_3 (2-CH_3/CF_3)

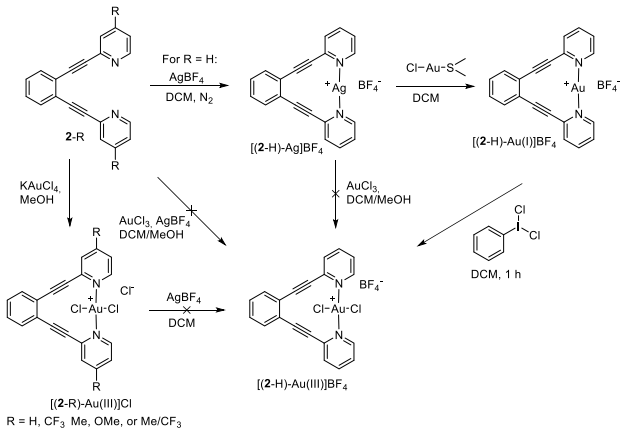

This bidentate ligand, and its close structural analogues, have earlier been successfully utilized in palladium,[45–49] mercury,[50] copper,[51] silver, and halonium complexes,[41,52–56] making its application in Au(III) chemistry plausible. Coordination of $KAuCl_4$ with **2**-H readily took place, resulting in precipitation of $[(2\text{-H})\text{-Au(III)}]Cl$ upon mixing in methanol (Scheme 1). Given its poor solubility in a wide range of solvents, we also prepared $[(2\text{-H})\text{-Au(III)}]BF_4$ from the corresponding Au(I) complex, $[(2\text{-H})\text{Au(I)}]BF_4$, by oxidation using dichloro(phenyl)-λ^3-iodane (Scheme 1).[57] Notably, the $[(2\text{-H})\text{-Au(III)}]BF_4$ complex could not be formed via an anion exchange with $[(2\text{-H})\text{-Au(III)}]Cl$. The $[(2\text{-H})\text{-Au(III)}]Cl$ and $[(2\text{-H})\text{-Au(III)}]BF_4$ complexes both catalyzed the cyclopropanation

Table 2. Experimental $\delta^{15}N$ and $\Delta\delta^{15}N_{coord}$ NMR Chemical Shifts in CD_2Cl_2, Calculated Au–N Bond Length, Calculated Changes of the Total Electron Population of the Pyridine Nitrogen $\Delta n(N)$ upon Substitution: as Estimated by Natural Atomic Populations Analysis for Pyridine Ligands 1-R and the Calculated Stabilization Energies of Bis(pyridine) Au(I) and Au(III) Complexes of Pyridine Ligands 1-R[a]

complex	$\delta\ ^{15}N_{complex}$	$\delta^{15}N_{ligand}$	$\Delta\delta^{15}N_{coord}$	Au–N bond length [Å]	$10^3\Delta n(N)$	ΔG_{stab}[b] [kcal/mol]
$[(1\text{-H})_2\text{-Au(I)}]BF_4$	−155.6	−67.0	−88.6	2.056		
$[(1\text{-H})_2\text{-Au(III)}]Cl$	−154.2	−67.0	−87.2	2.046	0.0	0.0
$[(1\text{-CF}_3)_2\text{-Au(III)}]Cl$	−144.1	−58.0	−86.1	2.047	−17.0	10.4
$[(1\text{-CH}_3)_2\text{-Au(III)}]Cl$	−162.6	−71.6	−91.0	2.044	8.0	−1.9
$[(1\text{-OCH}_3)_2\text{-Au(III)}]Cl$	−178.2	−86.0	−92.2	2.042	27.0	−2.7

[a]See the Supporting Information for computational details. [b]Calculated free energy change of the $[(1\text{-H})_2\text{-Au(III)}]^+ + 2 \times 1\text{-R} \rightarrow [(1\text{-R})_2\text{-Au(III)}]^+ + 2 \times 1\text{-H}$ isodesmic reaction.

https://dx.doi.org/10.1021/jacs.0c01941
J. Am. Chem. Soc. 2020, 142, 6439–6446

reaction, giving full conversion within 5 h (Table 3, entries 1 and 2). Despite its somewhat lower reactivity as compared to the analogous bis(pyridine) complex [(**1**-H)$_2$-Au(III)]Cl (Table 1, entry 1), this observation proves, for the first time, that Au(III) complexes of *trans*-chelating bidentate ligands are catalytically active.

Table 3. Reactivity of the [(2-R)-Au(III)]$^+$ and [(2-H)-Au(I)]$^+$ Complexes in the Cyclopropanation Reaction

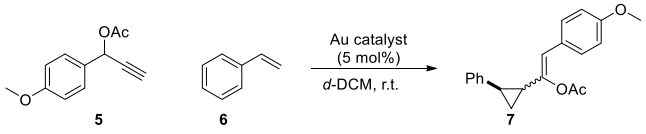

entry	Au catalyst	reaction time	conv [%] (*trans*:*cis*)
1	[(**2**-H)-Au(III)]BF_4	5 h	100 (23:77)
2	[(**2**-H)-Au(III)]Cl	5 h	100 (21:79)
3	[(**2**-CF_3)-Au(III)]Cl	30 min	100 (17:83)
4	[(**2**-CH_3)-Au(III)]Cl	10 h	41 (24:76)
5	[(**2**-OCH_3)-Au(III)]Cl	10 h	75 (18:82)
6	[(**2**-CH_3/CF_3)-Au(III)]Cl	10 h	8 (<1:>99)
7	[(**2**-H)-Au(I)]BF_4	12 h	40 (26:74)

The lower reactivity of [(**2**-H)-Au(III)]Cl may be explained by the stronger coordination of Au(III) to **2**-H as compared to pyridine (**1**-H), reflected by the 24 ppm smaller $|\Delta\delta^{15}N_{coord}|$ of [(**1**-H)$_2$-Au(III)]Cl (87.2 ppm, Table 2) as compared to [(**2**-H)-Au(III)]Cl (111.2 ppm, Table 4). This different coordination strength is corroborated by the calculated shorter N−Au distance of [(**2**-H)-Au(III)]Cl, 2.037 Å (Table 4) as compared to [(**1**-H)$_2$-Au(III)]Cl, 2.046 Å (Table 2). The 4-substituted analogues [(**2**-R)-Au(III)]Cl were prepared by following same the method described for [(**2**-H)-Au(III)]Cl and showed higher solubility in dichloromethane. The electron-poor [(**2**-CF_3)-Au(III)]Cl and the asymmetric [(**2**-CH_3/CF_3)-Au(III)]Cl complex were less stable than [(**2**-H)-Au(III)]Cl as judged from their stability in a dichloromethane solution monitored by ^{1}H NMR and confirmed by DFT computations (Table 4). The reactivity order of complexes [(**2**-R)-Au(III)]Cl followed the same trend in the cyclopropanation model reaction (Table 3) as the [(**1**-R)$_2$-Au(III)]Cl complexes (Table 1). This suggests that the geometrically restrained pyridine complexes react with the same mechanism as the unrestrained ones. Accordingly, the $\Delta\delta^{15}N_{coord}$ of [(**2**-R)-Au(III)]Cl (Table 4) showed linear correlation to the σ_{para} Hammett substituent constant (Figure 2), indicating that the reactivity of pyridine complexes is systematically modulated by electron density. A similar correlation was observed for [(**1**-R)$_2$-Au(III)]Cl complexes (Table 2).

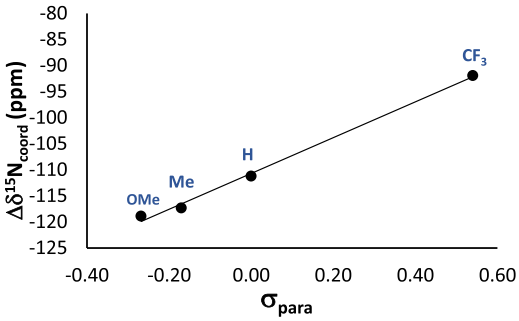

Figure 2. Correlation of the Hammett substituent constant and the $\Delta\delta^{15}N_{coord}$ shift of the [(**2**-R)-Au(III)]Cl complexes. R^2 = 0.99.

This experimental finding is supported by the variation of the net atomic charge of the pyridine nitrogen atom upon *para* substitution, as obtained by natural atomic population (NAP) analysis,[58] being well-correlated to the $\Delta\delta^{15}N_{coord}$ of pyridine complexes (Table 2; for details see the Supporting Information).

Whereas [(**2**-H)-Au(III)]Cl is less reactive (100% in 5 h) than [(**1**-H)$_2$-Au(III)]Cl (100% in <1 h), [(**2**-H)-Au(I)]BF_4 shows higher reactivity (40% in 12 h) than its unrestrained analogue [(**1**-H)$_2$-Au(I)]BF_4 (<5% in 2 h). The $\Delta\delta^{15}N_{coord}$ of [(**1**-H)$_2$-Au(I)]BF_4 (−88.6 ppm, Table 2) is comparable yet somewhat larger than that of [(**2**-H)-Au(I)]BF_4 (−85.6 ppm, Table 4), and the Au(I)−N bond length of the conformationally adjustable **1**-H complex is somewhat shorter (2.056 Å) than that of the geometrically restricted complex of **2**-H (2.064 Å). This suggests that a weak geometrical restraint that enforces weaker than optimal coordination of pyridine promotes the reactivity of Au(I). This is significant as pyridine is widely accepted to deactivate Au(I), and thus the reactivity of [(**2**-H)-Au(I)]BF_4 in cyclopropanation is unprecedented. This chelating ligand design could pave the way for the development of new types of catalytically active Au(I) complexes in organic reactions.

The DFT calculated Au−N bond lengths of the complexes [(**1**-H)$_2$-Au(III)]Cl (2.046 Å) and [(**2**-H)-Au(III)]Cl (2.037

Table 4. Experimental δ^{15}N and $\Delta\delta^{15}N_{coord}$ NMR Chemical Shifts CD_2Cl_2, Calculated Au−N Bond Length, and Calculated Changes of the Total Electron Population of the Pyridine Nitrogen Δn(N) upon Substitution: as Estimated by Natural Atomic Populations Analysis for Ligands 2-R

complex	δ 15Ncomplex	δ $^{15}N_{ligand}$	$\Delta\delta$ $^{15}N_{coord}$	Au−N bond length [Å]	ΔG_{stab} [a] [kcal/mol]
[(**2**-H)-Au(III)]Cl[b]	−179.8[b]	−63.6[b]	−111.2[b]	2.037	0.0
[(**2**-H)-Au(III)]BF_4[c]	−178.9[c]	−75.0[c]	−103.9[c]	2.037	0.0
[(**2**-CF_3)-Au(III)]Cl	−142.6	−50.7	−91.9	2.037	7.3
[(**2**-CH_3)-Au(III)]Cl	−186.5	−69.2	−117.3	2.035	−3.1
[(**2**-OCH_3)-Au(III)]Cl	−202.4	−83.5	−118.9	2.034	−4.8
[(**2**-CH_3/CF_3)-Au(III)]Cl	-159.5	−53.8	−105.7	2.042	2.0
	−189.5	−71.8	−117.7	2.030	
[(**2**-H)-Au(I)]BF_4	−150.1	−64.5	−85.6	2.064	−[d]
[(**2**-H)-Au(I)]BF_4[c]	−151.3[c]	−75.0[c]	−76.3[c]	2.064	−[d]

[a]Energies are given as stabilization energies relative to [Au(III)(**2**-H)]Cl. [b]Acquired in DMSO-d_6. [c]Acquired in methanol-d_4. [d]Not relevant to compare to the Au(III) complex due to lack of the two coordinating chlorides.

https://dx.doi.org/10.1021/jacs.0c01941
J. Am. Chem. Soc. 2020, 142, 6439−6446

Å) are shorter than the corresponding bond lengths of the analogous Au(I) complexes (Tables 2 and 4), in agreement with Au(III) being smaller and more electrophilic than Au(I). Overall, the reactivity of both Au(I) and Au(III) complexes appears to be a function of coordination strength. Weaker coordination results in higher catalytically activities and is associated with longer Au−N bond lengths and smaller $|\Delta\delta^{15}N_{coord}|$.

In an attempt to evaluate whether an asymmetric coordination of the nitrogen ligands with a *trans*-bis(pyridine)-Au(III) complex could be advantageous for catalytic activity, we synthesized the asymmetrically substituted complex [(**2**-CH_3/CF_3)-Au(III)]Cl. The different bond strengths of the electron-poor and the electron-rich pyridines were confirmed by the two Au−N bond lengths, as calculated by DFT, 2.042 and 2.030 Å, respectively (Table 4), with these bond lengths being longer and shorter than those of the corresponding symmetric complexes [(**2**-CH_3)-Au(III)]Cl (2.035 Å) and [(**2**-CF_3)-Au(III)]Cl (2.037 Å). The different strength of the Au−N bonds in the asymmetric complex is corroborated by different $|\Delta\delta^{15}N_{coord}|$ shifts of the two nitrogens (Table 4). The $|\Delta\delta^{15}N_{coord}|$ of the electron-rich pyridine of [(**2**-CH_3/CF_3)-Au(III)]Cl (117.7 ppm) is comparable to the $|\Delta\delta^{15}N_{coord}|$ of the corresponding symmetric complex [(**2**-CH_3)-Au(III)]Cl (117.3 ppm), whereas the $|\Delta\delta^{15}N_{coord}|$ of the CF_3 substituted pyridine (105.7) is larger than its corresponding symmetric complex [(**2**-CF_3)-Au(III)]Cl (91.9 ppm) (Table 4). This suggests that dissociation of the weaker coordinative Au−N bond, which is the one to the 4-trifluoromethylpyridine, is less favored than dissociation of the corresponding bond of [(**2**-CF_3)-Au(III)]Cl. Accordingly, [(**2**-CH_3/CF_3)-Au(III)]Cl shows lower catalytic activity in cyclopropanation (8% in 10 h) than [(**2**-CF_3)-Au(III)]Cl (100% in 30 min, Table 3). The Au−N bond dissociation may thus play a key role in the mechanism of Au(III)-mediated cyclopropanation.

To gain insights into the mechanism, we computed the Gibbs free energy profile for the envisioned intermediates and the related transition state of the key reaction between [(**1**-$H)_2$-Au(III)]Cl and propargyl ester (**5**) as shown in Figure 3 (see computational details in the Supporting Information). The reaction necessitates coordination of the substrate, which presumes decoordination of one of the four Lewis bases of the tetracoordinate Au(III) species. DFT calculations predict the decoordination of a pyridine to be vastly more favored ($\Delta\Delta G$ > 20 kcal/mol) over that of a chloride. The most favored structure of the proposed reaction intermediate, formed upon the exchange of a pyridine with propargyl ester **5**, has chlorides in a *cis* arrangement (intermediate **A**, Figure 3). This intermediate is predicted to be fairly unstable (ΔG = 23.2 kcal/mol) with respect to the $[(\mathbf{1}\text{-R})_2\text{-Au(III)}]^+$ + **5** reactant state; however, it is extremely reactive and easily initiates the 1,2-acyloxy migration process after rotation of the ester to form the transition state (**TS**). This computationally identified transition state (**TS**, Figure 3) is at 24.4 kcal/mol relative to the reactants and leads to the energetically low-lying cyclic intermediate **B** (for details, see the Supporting Information). Importantly, the energy barrier represented by this transition state, **TS**, varies upon the electronic nature of the pyridine 4-substituent. The energy order of **1**-CF_3 < **1**-H < **1**-CH_3 < **1**-OCH_3 is in qualitative agreement with the experimentally observed reactivity order of the [(**1**-$R)_2$-Au(III)] complexes (Table 1).

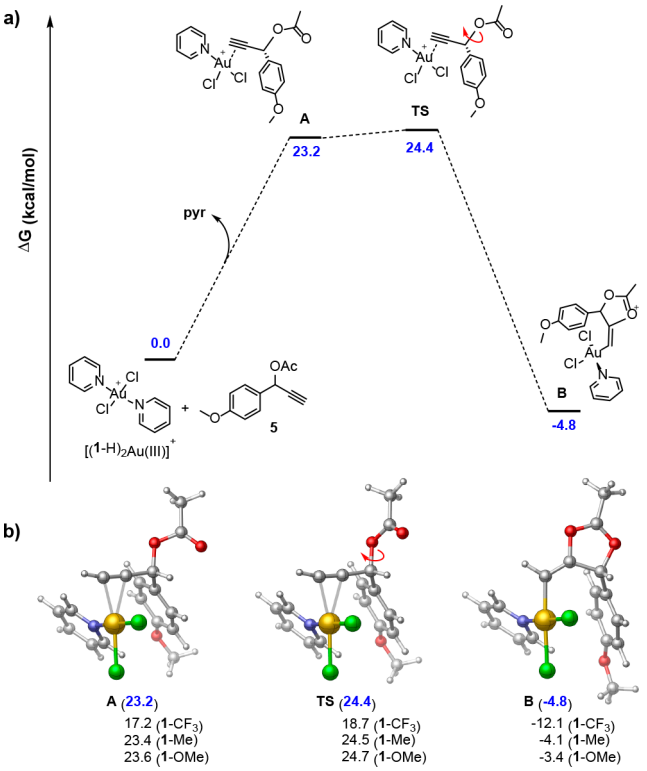

Figure 3. (a) Free energy data predicted for reactive intermediate **A**, transition state **TS** initiating the 1,2-acyloxy migration process, and subsequent cyclic intermediate **B** identified computationally for the reaction between $[(\mathbf{1}\text{-H})_2\text{-Au(III)}]^+$ and propargyl ester **5**. Relative stabilities (in kcal/mol) are shown in blue with respect to the $[(\mathbf{1}\text{-H})_2\text{-Au(III)}]^+$ + **5** reactant state. (b) Optimized structures of **A**, **TS**, and **B**. Energy data obtained for the analogous reactions with **1**-R = **1**-CF_3, **1**-CH_3, and **1**-OCH_3 are shown before the labels. Details for DFT calculation are given in the Supporting Information.

As we observed weaker coordination to increase the catalytic activity, the Au(III) complex of **3** (Figure 1) was investigated because this ligand was expected to enforce a longer nitrogen−nitrogen distance (Scheme 2, bottom left) and thereby expectably a weaker coordination to Au(III). Following the synthetic route described for the generation of [(**1**-$H)_2$-Au(III)]Cl, a mixture of two complexes possessing comparable $\Delta\delta^{15}N_{coord}$, that is, −81.4 ppm [**3**-$Au(III)_2$] and −80.8 ppm [**3**-$Au(III)]_2Cl_2$, was formed. The complex [**3**-$Au(III)_2$] was isolated by crystallization and identified by single-crystal X-ray crystallography. Instead of the expected 1:1 ligand to gold stoichiometry, the structure features two Au(III) ions for every ligand (Scheme 2). This complex gave full conversion in the cyclopropanation reaction within 10 h, thus showing a decreased reaction rate as compared to the Au(III) complexes of **1**-H (Table 1) and 2-H (Table 3). The lower reactivity of [**3**-$Au(III)_2$] (10 mol % Au(III), full conversion in 10 h) is in agreement with a decreased reactivity of Au(III) complexes that do not allow easy decoordination of a nitrogenous ligand.[59] Because of the lack of a suitable single crystal for the second ligated complex of **3**, DFT calculations were performed to identify plausible structures. The monomeric [**3**-Au(III)]Cl (Scheme 2b), possessing a bis-coordinated Au(III) center analogous to [**2**-Au(III)]Cl, is highly strained and unstable as compared to dimeric structures that have two N−Au−N bridges (Scheme 2). Out of the possible dimeric geometries, [**3**-$Au(III)]_2Cl_2$ was found to be the most stable (Supporting

https://dx.doi.org/10.1021/jacs.0c01941
J. Am. Chem. Soc. 2020, 142, 6439−6446

Scheme 2. Conditions for Coordination of Au(III) by 3 and (a) the Complex Identified by X-ray Analysis, [3-Au(III)$_2$] Complex, and (b) Computationally Identified Monomeric and Dimeric Forms of Complex [3-Au(III)]$_2$Cl$_2$[a]

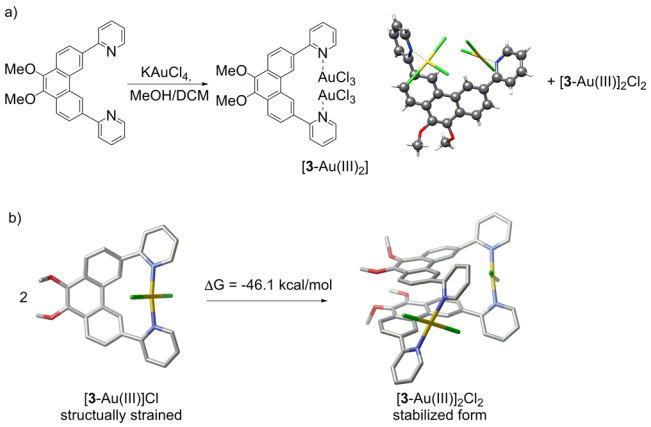

[a]The free energy of dimerization (ΔG) is shown above the arrow. Hydrogen atoms are omitted for clarity. Details for DFT calculation are given in the Supporting Information.

Information), presumably due to the advantageous π-stacking of its phenanthrenes.

To evaluate whether horizontal twisting of the coordination plane of the N−Au−N interaction may modulate the catalytic activity of Au(III), we mixed the bidentate ligand **4** with $AuCl_3$ (Scheme 3). Crystals suitable for X-ray analysis were grown by slow diffusion of *n*-pentane into a dichloromethane solution. Formation of a dimeric helix, [**4**-Au(I)]$_2$(AuCl$_4$)$_2$, associated

Scheme 3. Coordination Condition for Formation of (a) [4-Au(I)]$_2$(AuCl$_4$)$_2$ by Addition of the Ligand 4 Dissolved in Dichloromethane to $AuCl_3$ Dissolved in Methanol and (b) [4-Au(I)]$_2$(BF$_4$)$_2$ Starting from Chloro(dimethyl sulfide)gold(I) and $AgBF_4$ in Dichloromethane[a]

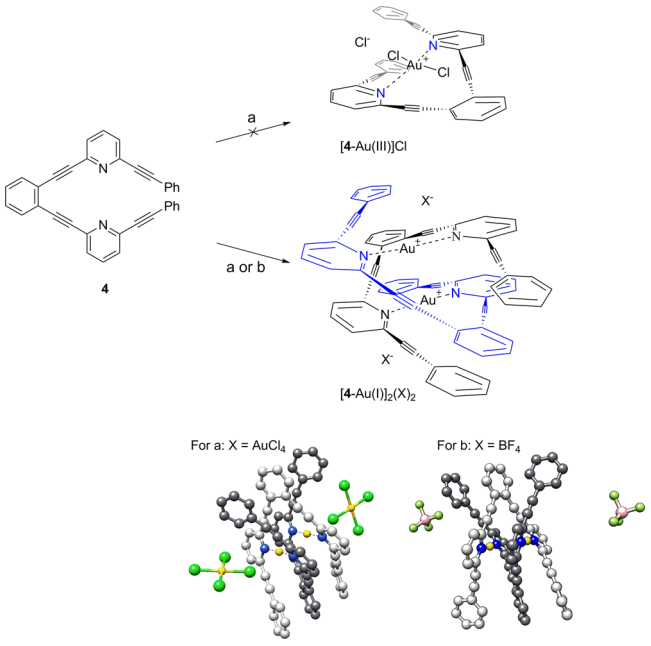

[a]Crystal structures of complexes formed with two different counterions are depicted at the bottom of the scheme.

with partial reduction of Au(III) to Au(I) was revealed by single-crystal X-ray crystallography. Hence, Au(I) was observed to coordinate to ligand **4** and $AuCl_4^-$ to act as a counterion. Upon coordination of Au(I) to ligand **4**, starting from chloro(dimethyl sulfide)Au(I) and $AgBF_4$, the analogous [**4**-Au(I)]$_2$(BF$_4$)$_2$ complex was obtained (Scheme 3). The $\Delta\delta^{15}N_{coord}$ of −83.2 for [**4**-Au(I)]$_2$(BF$_4$)$_2$ was slightly smaller than the coordination shift of [(**1**-H)$_2$-Au(I)]BF$_4$ and [(**2**-H)-Au(I)]BF$_4$, confirming the weaker coordination of Au(I) to **4** as compared to **1**-H and **2**-H (Tables 2 and 4). Formation of the dimeric helical [**4**-Au(I)]$_2$ geometry allows close to linear N−Au−N interactions (176.6°) and optimal Au(I)−N bond lengths (2.01 Å) and thus avoids horizontal twisting that would have been enforced in a [**4**-Au(III)]Cl single-helix geometry (Scheme 3a).

Ligand **4** has been reported to form a monomeric helix when coordinating iodine(I) [**4**-I(I)]BF$_4$.[42] The difference in topology of the [**4**-Au(I)]$_2$(BF$_4$)$_2$ dimeric helix from [**4**-I(I)]BF$_4$ (Scheme 4) is corroborated by DFT calculations,

Scheme 4. Computational (DFT) Investigation of the Relative Stability of Monomeric and Dimeric Helical Structures of 4 in Complexes with Au(I) and I(I) Reveal Opposite Preferences, Corroborating the Experimental Observations[a]

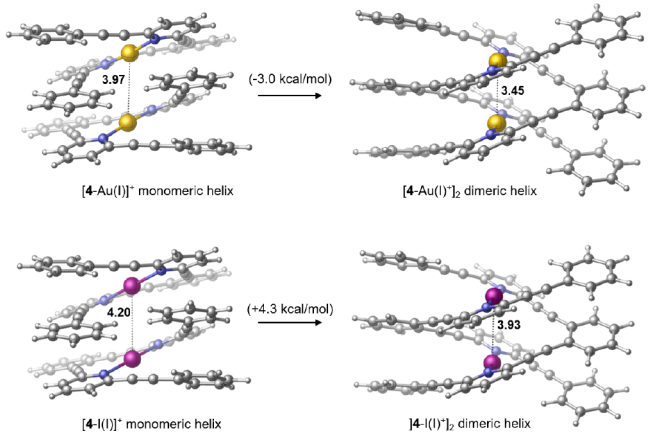

[a]Thus, Au(I) prefers to form a dimeric, whereas I(I) a monomeric helix. Energy values shown in parentheses refer to the free energy changes for the interconversion of the monomeric and dimeric geometries. Distances between the Au(I) and I(I) centers are given in Å. Details for the DFT calculation are given in the Supporting Information.

which show a thermodynamic preference for formation of a dimeric, double-helical structure for [**4**-Au(I)]$_2$(BF$_4$)$_2$ over a monomeric helical complex. This is most plausibly explained by stronger π-stacking interactions in the double helical [**4**-Au(I)]$_2$(BF$_4$)$_2$ geometry due to the smaller van der Waals radius of Au(I) as compared to I(I), which favors the monomeric helical structure (for details, see the Supporting Information).

The [**4**-Au(I)]$_2$(AuCl$_4$)$_2$ complex gave full conversion within 1 h as catalyst for the cyclopropanation model reaction, whereas barely 19% conversion was obtained within 24 h for the analogous [**4**-Au(I)]$_2$(BF$_4$)$_2$. This reveals the $AuCl_4^-$ counterion of the former complex is primarily responsible for the catalytic activity, whereas the Au(I) within the complex has a low catalytic activity. This is in excellent agreement with the

https://dx.doi.org/10.1021/jacs.0c01941
J. Am. Chem. Soc. 2020, 142, 6439−6446

low catalytic activity of $[(\mathbf{1}\text{-H})_2\text{-Au(I)}]BF_4$ (Table 1). The reactivity order $[(\mathbf{1}\text{-H})_2\text{-Au(I)}]BF_4 < [\mathbf{4}\text{-Au(I)}]_2(BF_4)_2 < [(\mathbf{2}\text{-H})\text{-Au(I)}]BF_4$ suggests that the catalytic activity of bis(pyridine)Au(I) complexes is modulated by the geometric strain of the N−Au−N three-center bond.

CONCLUSION

Bis(pyridine)Au(III) complexes are applicable as catalysts as shown by using the cyclopropanation of styrene (**6**) with propargyl ester (**5**) as a model reaction. By systematic NMR spectroscopic, X-ray crystallographic, and computational assessment of a series of structurally related complexes, we demonstrated that the electron density of the pyridine ligands has a pivotal influence on the catalytic activity of Au(III). Accordingly, the energy requirement of the formation of a key intermediate and the subsequent transition state is predicted by DFT to depend on the electron density of the nitrogen of the pyridine ligand. The catalytic activity of geometrically restrained *trans*-bis(pyridine)Au(III) complexes was investigated here for the first time. These complexes also show electron-density-dependent reactivity, which is somewhat lower than that of the Au(III) complexes of free pyridines. DFT calculations suggest that these types of complexes convert into a *cis*-dichlorido(pyridine)Au(III) intermediate upon decoordination of a pyridyl functionality. Geometrical restriction of bis(pyridine)-type ligands enforced increased strain in the N−Au−N bond, resulting in the formation of a variety of dimeric structures, including among others an unusual double-helical supramolecular assembly. Whereas cyclopropanations initiated with bis(pyridine)Au(III) complexes are shown to be Au(III)-mediated reactions, the lower yet significant catalytic activity of bis(pyridine)Au(I) complexes is demonstrated here for the very first time. The reactivity appears to be modulated by strain and thus is expected to be tunable.

Despite a quickly growing interest in Au(III) catalysis, its understanding lags behind that of transition metal catalysis in general. So far, the mechanism of most Au(III)-catalyzed reactions is not well understood. Furthermore, systematic, combined spectroscopic and theoretical investigations of the mechanism of Au(III)-mediated reactions are rare. This work is expected to contribute to providing the basis of an improved understanding of Au(III) chemistry and the development of new, robust synthetic methodologies.

ASSOCIATED CONTENT

Supporting Information

The Supporting Information is available free of charge at https://pubs.acs.org/doi/10.1021/jacs.0c01941.

Details on the synthesis and spectroscopic data for compound identification and details on the NMR, computational, and X-ray diffractometric investigations (PDF)

The X-ray structure of compound $[4\text{-Au(I)}]_2(BF_4)_2$ (CIF)

The X-ray structure of compound $[4\text{-Au(I)}]_2(AuCl_4)_2$ (CIF)

The X-ray structure of compound $[3\text{-Au(III)}]_2Cl_2$ (CIF)

AUTHOR INFORMATION

Corresponding Authors

Máté Erdélyi − *Department of Chemistry, BMC Uppsala University, 752 37 Uppsala, Sweden;* orcid.org/0000-0003-0359-5970; Email: mate.erdelyi@kemi.uu.se

Imre Pápai − *Institute of Organic Chemistry, Research Centre for Natural Sciences, H1117 Budapest, Hungary; Department of Chemistry, University J. Selyeho, 94505 Komárno, Slovakia;* orcid.org/0000-0002-4978-0365; Email: papai.imre@ttk.mta.hu

Authors

Ann Christin Reiersølmoen − *Department of Chemistry, Norwegian University of Science and Technology, 7491 Trondheim, Norway;* orcid.org/0000-0001-9840-2769

Dániel Csókás − *Institute of Organic Chemistry, Research Centre for Natural Sciences, H1117 Budapest, Hungary;* orcid.org/0000-0002-4150-477X

Sigurd Øien-Ødegaard − *Centre for Material Sciences and Nanotechnology, University of Oslo, 0371 Oslo, Norway;* orcid.org/0000-0001-7913-4199

Alan Vanderkooy − *Department of Chemistry, BMC Uppsala University, 752 37 Uppsala, Sweden;* orcid.org/0000-0002-0532-9118

Arvind Kumar Gupta − *Department of Organic Chemistry − Ångström Laboratory, Uppsala University, 751 20 Uppsala, Sweden;* orcid.org/0000-0002-8969-1236

Anna-Carin C. Carlsson − *Department of Chemistry and Molecular Biology, University of Gothenburg, SE-412 96 Gothenburg, Sweden;* orcid.org/0000-0003-1099-5681

Andreas Orthaber − *Department of Organic Chemistry − Ångström Laboratory, Uppsala University, 751 20 Uppsala, Sweden;* orcid.org/0000-0001-5403-9902

Anne Fiksdahl − *Department of Chemistry, Norwegian University of Science and Technology, 7491 Trondheim, Norway;* orcid.org/0000-0003-2577-2421

Complete contact information is available at: https://pubs.acs.org/10.1021/jacs.0c01941

Notes

The authors declare no competing financial interest.

ACKNOWLEDGMENTS

This work was supported by the Research Council of Norway and has been performed with the support from the Anders Jahres Fond. The project made use of the NMR Uppsala infrastructure, which is funded by the Department of Chemistry - BMC and the Disciplinary Domain of Medicine and Pharmacy. It was also supported by the European Regional Development Fund via the "Support of research and development capacities in the area of nanochemical and supramolecular systems" project (code: 313011T583). We thank Sofia Lindblad (Uppsala University) for donation of ligands **2**-CH_3/CF_3 and **3**.

REFERENCES

(1) Hashmi, A. S. K. Gold-Catalyzed Organic Reactions. *Chem. Rev.* **2007**, *107*, 3180−3211.

(2) Jiménez-Núñez, E.; Echavarren, A. M. Gold-Catalyzed Cycloisomerizations of Enynes: A Mechanistic Perspective. *Chem. Rev.* **2008**, *108*, 3326−3350.

(3) Fukuda, Y.; Utimoto, K. Effective Transformation of Unactivated Alkynes into Ketones or Acetals with a Gold(III) Catalyst. *J. Org. Chem.* **1991**, *56*, 3729−3731.
(4) Hashmi, A. S. K.; Schwarz, L.; Choi, J.-H.; Frost, T. M. A New Gold-Catalyzed C−C Bond Formation. *Angew. Chem., Int. Ed.* **2000**, *39*, 2285−2288.
(5) Hashmi, A. S. K.; Frost, T. M.; Bats, J. W. Highly Selective Gold-Catalyzed Arene Synthesis. *J. Am. Chem. Soc.* **2000**, *122*, 11553−11554.
(6) Hashmi, A. S. K.; Blanco, M. C.; Fischer, D.; Bats, J. W. Gold Catalysis: Evidence for the in-Situ Reduction of Gold(III) During the Cyclization of Allenyl Carbinols. *Eur. J. Org. Chem.* **2006**, *2006*, 1387−1389.
(7) Yang, Y.; Antoni, P.; Zimmer, M.; Sekine, K.; Mulks, F. F.; Hu, L.; Zhang, L.; Rudolph, M.; Rominger, F.; Hashmi, A. S. K. Dual Gold/Silver Catalysis Involving Alkynylgold(III) Intermediates Formed by Oxidative Addition and Silver-Catalyzed C−H Activation for the Direct Alkynylation of Cyclopropenes. *Angew. Chem., Int. Ed.* **2019**, *58*, 5129−5133.
(8) Rodriguez, J.; Adet, N.; Saffon-Merceron, N.; Bourissou, D. Au(I)/Au(III)-Catalyzed C−N Coupling. *Chem. Commun.* **2020**, *56*, 94−97.
(9) Zhang, Q.; Zhang, Z.-Q.; Fu, Y.; Yu, H.-Z. Mechanism of the Visible Light-Mediated Gold-Catalyzed Oxyarylation Reaction of Alkenes. *ACS Catal.* **2016**, *6*, 798−808.
(10) Yang, Y.; Eberle, L.; Mulks, F. F.; Wunsch, J. F.; Zimmer, M.; Rominger, F.; Rudolph, M.; Hashmi, A. S. K. Trans Influence of Ligands on the Oxidation of Gold(I) Complexes. *J. Am. Chem. Soc.* **2019**, *141*, 17414−17420.
(11) Schmidbaur, H.; Schier, A. Gold(III) Compounds for Homogeneous Catalysis: Preparation, Reaction Conditions, and Scope of Application. *Arab. J. Sci. Eng.* **2012**, *37*, 1187−1225.
(12) Zou, T.; Lum, C. T.; Lok, C.-N.; Zhang, J.-J.; Che, C.-M. Chemical Biology of Anticancer Gold(III) and Gold(I) Complexes. *Chem. Soc. Rev.* **2015**, *44*, 8786−8801.
(13) Tian, X.; Song, L.; Rudolph, M.; Rominger, F.; Hashmi, A. S. K. Synthesis of 2-Aminoindoles through Gold-Catalyzed C−H Annulations of Sulfilimines with N-Arylynamides. *Org. Lett.* **2019**, *21*, 4327−4330.
(14) Jiang, J.-J.; Cui, J.-F.; Yang, B.; Ning, Y.; Lai, N. C.-H.; Wong, M.-K. Chiral Cyclometalated Oxazoline Gold(III) Complex-Catalyzed Asymmetric Carboalkoxylation of Alkynes. *Org. Lett.* **2019**, *21*, 6289−6294.
(15) Reiersølmoen, A. C.; Østrem, E.; Fiksdahl, A. Gold(III)-Catalysed Cis-to-Trans Cyclopropyl Isomerization. *Eur. J. Org. Chem.* **2018**, *2018*, 3317−3325.
(16) Nair, A. G.; McBurney, R. T.; Gatus, M. R. D.; Binding, S. C.; Messerle, B. A. Gold(III) NHC Complexes for Catalyzing Dihydroalkoxylation and Hydroamination Reactions. *Inorg. Chem.* **2017**, *56*, 12067−12075.
(17) Bohan, P. T.; Toste, F. D. Well-Defined Chiral Gold(III) Complex Catalyzed Direct Enantioconvergent Kinetic Resolution of 1,5-Enynes. *J. Am. Chem. Soc.* **2017**, *139*, 11016−11019.
(18) Belmonte Sánchez, E.; Iglesias, M. J.; el Hajjouji, H.; Roces, L.; García-Granda, S.; Villuendas, P.; Urriolabeitia, E. P.; López Ortiz, F. Cycloaurated Phosphinothioic Amide Complex as a Precursor of Gold(I) Nanoparticles: Efficient Catalysts for A3 Synthesis of Propargylamines under Solvent-Free Conditions. *Organometallics* **2017**, *36*, 1962−1973.
(19) Wong, K.-F.; Deng, J.-R.; Wei, X.-Q.; Shao, S.-P.; Xiang, D.-P.; Wong, M.-K. Visual Detection of Formaldehyde by Highly Selective Fluorophore Labeling Via Gold(III) Complex-Mediated Three-Component Coupling Reaction. *Org. Biomol. Chem.* **2015**, *13*, 7408−7411.
(20) Chen, T.; Cai, C. Catalytic Hydration of Alkynes to Ketones by a Salen−Gold(III) Complex. *Catal. Commun.* **2015**, *65*, 102−104.
(21) Li, D.; Rao, W.; Tay, G. L.; Ayers, B. J.; Chan, P. W. H. Gold-Catalyzed Cycloisomerization of 1,6-Diyne Esters to 1h-Cyclopenta-[B]Naphthalenes, Cis-Cyclopenten-2-Yl Δ-Diketones, and Bicyclo[3.2.0]Hepta-1,5-Dienes. *J. Org. Chem.* **2014**, *79*, 11301−11315.
(22) Xue, Q.; Xie, J.; Jin, H.; Cheng, Y.; Zhu, C. Highly Efficient Visible-Light-Induced Aerobic Oxidative C−C, C−P Coupling from C−H Bonds Catalyzed by a Gold(III)-Complex. *Org. Biomol. Chem.* **2013**, *11*, 1606−1609.
(23) Corma, A.; Domínguez, I.; Doménech, A.; Fornés, V.; Gómez-García, C. J.; Ródenas, T.; Sabater, M. J. Enantioselective Epoxidation of Olefins with Molecular Oxygen Catalyzed by Gold(III): A Dual Pathway for Oxygen Transfer. *J. Catal.* **2009**, *265*, 238−244.
(24) Wu, C.-Y.; Horibe, T.; Jacobsen, C. B.; Toste, F. D. Stable Gold(III) Catalysts by Oxidative Addition of a Carbon−Carbon Bond. *Nature* **2015**, *517*, 449−454.
(25) Yang, Y.; Hu, W.; Ye, X.; Wang, D.; Shi, X. Preparation of Triazole Gold(III) Complex as an Effective Catalyst for the Synthesis of E-A-Haloenones. *Adv. Synth. Catal.* **2016**, *358*, 2583−2588.
(26) Miura, Y.; Mochida, T.; Motodate, S.; Kato, K. Synthesis and Thermal Properties of Salts Comprising Cationic Bis(Oxazoline)-AuIII Complexes and Fluorinated Anions. *Polyhedron* **2016**, *113*, 1−4.
(27) Cinellu, M. A.; Maiore, L.; Minghetti, G.; Cocco, F.; Stoccoro, S.; Zucca, A.; Manassero, M.; Manassero, C. Gold(III) Adducts with Chiral Pyridinyl-Oxazolines. Synthesis, Reactivity of the Coordinated Ligands, and Structural Characterizations. *Organometallics* **2009**, *28*, 7015−7024.
(28) Rodriguez, J.; Bourissou, D. Well-Defined Chiral Gold(III) Complexes: New Opportunities in Asymmetric Catalysis. *Angew. Chem., Int. Ed.* **2018**, *57*, 386−388.
(29) Ko, H.-M.; Kung, K. K.-Y.; Cui, J.-F.; Wong, M.-K. Bis-Cyclometallated Gold(III) Complexes as Efficient Catalysts for Synthesis of Propargylamines and Alkylated Indoles. *Chem. Commun.* **2013**, *49*, 8869−8871.
(30) Kumar, R.; Nevado, C. Cyclometalated Gold(III) Complexes: Synthesis, Reactivity, and Physicochemical Properties. *Angew. Chem., Int. Ed.* **2017**, *56*, 1994−2015.
(31) Kung, K. K.-Y.; Ko, H.-M.; Cui, J.-F.; Chong, H.-C.; Leung, Y.-C.; Wong, M.-K. Cyclometalated Gold(III) Complexes for Chemoselective Cysteine Modification Via Ligand Controlled C−S Bond-Forming Reductive Elimination. *Chem. Commun.* **2014**, *50*, 11899−11902.
(32) Lo, V. K.-Y.; Liu, Y.; Wong, M.-K.; Che, C.-M. Gold(III) Salen Complex-Catalyzed Synthesis of Propargylamines Via a Three-Component Coupling Reaction. *Org. Lett.* **2006**, *8*, 1529−1532.
(33) Rajput, A.; Mukherjee, R. Coordination Chemistry with Pyridine/Pyrazine Amide Ligands. Some Noteworthy Results. *Coord. Chem. Rev.* **2013**, *257*, 350−368.
(34) Kwong, H.-L.; Yeung, H.-L.; Yeung, C.-T.; Lee, W.-S.; Lee, C.-S.; Wong, W.-L. Chiral Pyridine-Containing Ligands in Asymmetric Catalysis. *Coord. Chem. Rev.* **2007**, *251*, 2188−2222.
(35) Hashmi, A. S. K.; Weyrauch, J. P.; Rudolph, M.; Kurpejović, E. Gold Catalysis: The Benefits of N and N,O Ligands. *Angew. Chem., Int. Ed.* **2004**, *43*, 6545−6547.
(36) Hashmi, A. S. K.; Rudolph, M.; Weyrauch, J. P.; Wölfle, M.; Frey, W.; Bats, J. W. Gold Catalysis: Proof of Arene Oxides as Intermediates in the Phenol Synthesis. *Angew. Chem., Int. Ed.* **2005**, *44*, 2798−2801.
(37) Tomás-Mendivil, E.; Toullec, P. Y.; Díez, J.; Conejero, S.; Michelet, V.; Cadierno, V. Cycloisomerization Versus Hydration Reactions in Aqueous Media: A Au(III)-NHC Catalyst That Makes the Difference. *Org. Lett.* **2012**, *14*, 2520−2523.
(38) von Wachenfeldt, H.; Polukeev, A. V.; Loganathan, N.; Paulsen, F.; Röse, P.; Garreau, M.; Wendt, O. F.; Strand, D. Cyclometallated Gold(III) Aryl-Pyridine Complexes as Efficient Catalysts for Three-Component Synthesis of Substituted Oxazoles. *Dalton Trans.* **2015**, *44*, 5347−5353.
(39) Hashmi, A. S. K.; Lothschütz, C.; Ackermann, M.; Doepp, R.; Anantharaman, S.; Marchetti, B.; Bertagnolli, H.; Rominger, F. Gold Catalysis: In Situ Exafs Study of Homogeneous Oxidative Esterification. *Chem. - Eur. J.* **2010**, *16*, 8012−8019.

https://dx.doi.org/10.1021/jacs.0c01941
J. Am. Chem. Soc. 2020, 142, 6439−6446

(40) Zhang, Y.; Feng, B.; Zhu, C. Au(III)-Catalyzed Intermolecular Amidation of Benzylic C-H Bonds. *Org. Biomol. Chem.* **2012**, *10*, 9137−41.
(41) Carlsson, A.-C. C.; Mehmeti, K.; Uhrbom, M.; Karim, A.; Bedin, M.; Puttreddy, R.; Kleinmaier, R.; Neverov, A. A.; Nekoueishahraki, B.; Gräfenstein, J.; Rissanen, K.; Erdélyi, M. Substituent Effects on the $[N-I-N]^+$ Halogen Bond. *J. Am. Chem. Soc.* **2016**, *138*, 9853−9863.
(42) Vanderkooy, A.; Gupta, A. K.; Földes, T.; Lindblad, S.; Orthaber, A.; Pápai, I.; Erdélyi, M. Halogen Bonding Helicates Encompassing Iodonium Cations. *Angew. Chem.* **2019**, *131*, 9110−9114.
(43) Andersson, H.; Carlsson, A.-C. C.; Nekoueishahraki, B.; Brath, U.; Erdélyi, M. Solvent Effects on Nitrogen Chemical Shifts. *Annu. Rep. NMR Spectrosc.* **2015**, *86*, 73−210.
(44) Adams, H.-N.; Strähle, J. Die Pyridinaddukte Der Gold-halogenide. 1. Darstellung Und Struktur Von [Hpy][$AuCl_4$], $AuCl_3 \cdot$ Py, [$AuCl_2(Py)_2$]Cl · H_2O Und [$AuCl_2(Py)_2$][$AuCl_2$]. *Z. Anorg. Allg. Chem.* **1982**, *485*, 65−80.
(45) Pereira, F. A.; Fallows, T.; Frank, M.; Chen, A.; Clever, G. H. Stable and Metastable Self-Assembled Rings Based on Trans-Chelated Pdii. *Z. Anorg. Allg. Chem.* **2013**, *639*, 1598−1605.
(46) Atobe, S.; Sonoda, M.; Suzuki, Y.; Yamamoto, T.; Masuno, H.; Shinohara, H.; Ogawa, A. Palladium-Catalyzed Oxidative Homocoupling Reaction of Terminal Acetylenes Using Trans-Bidentatable 1-(2-Pyridylethynyl)-2-(2-Thienylethynyl)Benzene. *Res. Chem. Intermed.* **2013**, *39*, 359−370.
(47) Jung, M.; Suzaki, Y.; Saito, T.; Shimada, K.; Osakada, K. Pd Complexes with Trans-Chelating Ligands Composed of Two Pyridyl Groups and Rigid Π-Conjugated Backbone. *Polyhedron* **2012**, *40*, 168−174.
(48) Atobe, S.; Masuno, H.; Sonoda, M.; Suzuki, Y.; Shinohara, H.; Shibata, S.; Ogawa, A. Pd-Catalyzed Coupling Reaction of Acid Chlorides with Terminal Alkynes Using 1-(2-Pyridylethynyl)-2-(2-Thienylethynyl)Benzene Ligand. *Tetrahedron Lett.* **2012**, *53*, 1764−1767.
(49) Kawano, T.; Shinomaru, T.; Ueda, I. Highly Active Pd(II) Catalysts with Trans-Bidentate Pyridine Ligands for the Heck Reaction. *Org. Lett.* **2002**, *4*, 2545−2547.
(50) Barnes, C. L.; Bosch, E. Synthesis and X-Ray Crystal Structure of a Complex Formed by Reaction of 1,2-Bis(2′-Pyridylethynyl)-Benzene and Mercury(II) Chloride. *J. Chem. Crystallogr.* **2006**, *36*, 563−566.
(51) Bosch, E.; Barnes, C. L. Ligand Flexibility and Dual Complexation Modes on Reaction of 1,2- Bis (2′-Pyridylethynyl)-Benzene with Copper(I) Halides. *J. Coord. Chem.* **2003**, *56*, 329−336.
(52) Neverov, A. A.; Feng, H. X.; Hamilton, K.; Brown, R. S. Bis(Pyridine)-Based Bromonium Ions. Molecular Structures of Bis(2,4,6-Collidine)Bromonium Perchlorate and Bis(Pyridine)-Bromonium Triflate and the Mechanism of the Reactions of 1,2-Bis(2′-Pyridylethynyl)Benzenebrominum Triflate and Bis(Pyridine)-Bromonium Triflate with Acceptor Olefins. *J. Org. Chem.* **2003**, *68*, 3802−3810.
(53) Brennan, N. L.; Barnes, C. L.; Bosch, E. Complexation of Silver(I) Cation by a Series of Heterosubstituted Dipyridyl Ligands. *Inorg. Chim. Acta* **2010**, *363*, 3987−3992.
(54) Bedin, M.; Karim, A.; Reitti, M.; Carlsson, A.-C. C.; Topić, F.; Cetina, M.; Pan, F.; Havel, V.; Al-Ameri, F.; Sindelar, V.; Rissanen, K.; Gräfenstein, J.; Erdélyi, M. Counterion Influence on the N−I−N Halogen Bond. *Chem. Sci.* **2015**, *6*, 3746−3756.
(55) Lindblad, S.; Mehmeti, K.; Veiga, A. X.; Nekoueishahraki, B.; Gräfenstein, J.; Erdélyi, M. Halogen Bond Asymmetry in Solution. *J. Am. Chem. Soc.* **2018**, *140*, 13503−13513.
(56) Karim, A.; Schulz, N.; Andersson, H.; Nekoueishahraki, B.; Carlsson, A.-C. C.; Sarabi, D.; Valkonen, A.; Rissanen, K.; Gräfenstein, J.; Keller, S.; Erdélyi, M. Carbon's Three-Center, Four-Electron Tetrel Bond, Treated Experimentally. *J. Am. Chem. Soc.* **2018**, *140*, 17571−17579.
(57) Albayer, M.; Dutton, J. L. Synthesis of Cationic Gold(III) Complexes Using Iodine(III). *J. Coord. Chem.* **2019**, *72*, 1307−1321.
(58) Reed, A. E.; Weinstock, R. B.; Weinhold, F. Natural Population Analysis. *J. Chem. Phys.* **1985**, *83*, 735−746.
(59) Reiersølmoen, A. C.; Csokas, D.; Pápai, I.; Fiksdahl, A.; Erdélyi, M. The Mechanism of Au(III) Mediated Alkoxycyclization of a 1,6-Enyne. *J. Am. Chem. Soc.* **2019**, *141*, 18221−18229.

https://dx.doi.org/10.1021/jacs.0c01941
J. Am. Chem. Soc. 2020, 142, 6439−6446